Durability Performance of Concrete Incorporating Iron Ore Tailings

Shettima Umara Ali [1*], Hassan Ibrahim Ogiri [2], Amina Suleiman Gimba [1], Falamta Audu Mustapha[1]
[1]Department of Civil Engineering Technology, Federal Polytechnic Damaturu, 620221, Yobe State, Nigeria
[2]Department of Building Technology, Federal University of Technology, Minna, Niger state, Nigeria
** Corresponding author: alishettima2@gmail.com*

Abstract
Durability is the ability to last a long time without significant deterioration. A durable material helps the environment by conserving resources and reducing wastes and the environmental impacts of repair and replacement. Concrete resists weathering action, chemical attack, and abrasion while maintaining its desired engineering properties. Different concretes require different degrees of durability depending on the exposure environment and the properties desired. Concrete ingredients, their proportioning, interactions between them, placing and curing practices, and the service environment determine the ultimate durability and life of the concrete. Iron ore tailings are the solid waste discharged by the concentration plant after useful components is selected from the ore, which is an important source of environmental pollution in mining development. Iron ore tailings not only needs to occupy a lot of land and cause great harm to the surrounding ecological environment, but also needs to treatment and maintenance costs. River Sand is one of the constituents of concrete which was used as fine aggregate. However, consistent usage of sand in the construction industry contributes significantly to the depletion of natural resources. To achieve more sustainable and durable construction materials, this paper reports the durability performance of concrete incorporating IOT as sand replacement. Concrete with IOT of 0.40 and 0.60 w/c ratios were designed at 0%, 25%, 50%, 75% and 100% replacement by weight of river sand and exposed to chloride penetration, carbonation and acid attack. The possibility of corrosion prone was check through electrical resistivity of the concrete. Microstructure tests in terms of Thermo gravimetric analysis and differential thermal analysis (TGA/DTA) was conducted on IOT and river sand. Results showed that IOT affect mixture workability negatively. However, the inclusion of super plasticiser showed tremendous influence in increasing the workability and reduced this drawback. At 50% replacement, the compressive strength of the concrete at 90 days were 68.6 and 50.3 MPa for 0.40 and 0.60 w/c ratios, respectively. Concrete with IOT indicates a good resistance to carbonation compared to control specimen.

Keywords: *Iron ore tailings, River sand, Thermo gravimetric analysis and differential thermal analysis, Carbonation, Electrical resistivity,*

INTRODUCTION

The consumption of natural aggregate has been increased in recent years and if proper alternative were not provided, concrete industry will consume 8–12 billion tons of natural aggregate annually (Yaprak, Aruntas Huseyin Yılmaz, Demir Ilhami, Simsek Osman, & Gokhan., 2011). Such large consumption of natural aggregates will cause destruction of the environment. Therefore there is an urgent need to find and supply alternative substitutes for natural aggregates by exploring the possibility of utilization of industrial by-products and waste materials in making concrete. Iron ore tailings (IOT), an industrial waste, generated during the production of iron ore can be utilized in concrete to lessen the environmental problems. The use of industrial solid waste as a partial or full replacement of aggregate in construction activities not only saves land fill space but also reduces the demand for extraction of natural raw materials for future generations and this will lead to sustainable concrete and greener environment.

Durability of concrete is the ability of concrete to perform satisfactorily in the exposure condition to which it is subjected over an intended period of time with minimum of maintenance. Circumstances such as chloride penetration, acidic effect, carbonation etc. can lead to severe deterioration of concrete.

The rate of chloride ion penetration into concrete is a significant parameter that affects the durability of reinforced concrete structure especially when the structure is exposed to a marine environment, de-icing salts, or both (Yang & Chiang, 2008).

Carbonation of concrete is one of the major causes of corrosion of steel reinforcement and also one of the major factor in the degradation of concrete structures (Khunthongkeaw, Tangtermsirikul, & Leelawat, 2006). During cement hydration, large amounts of calcium hydroxide (CH) are released, thereby increasing the pH above 12.5 in the aqueous phase of the concrete. It has also been reported that carbon dioxide (CO_2) present in the atmosphere can penetrate the porous network of the concrete and reacts in the presence of moisture with calcium hydroxide and hydrated calcium silicates.

Acid mainly attacks concrete structures such as foundation, retaining wall, pavement, embankment and bridge deck thereby dissolving the constituent materials, leading to weakening of the strength of the affected concrete. Concrete structures in industrial zones are susceptible to deterioration due to acid rain of which sulphuric acid is a chief component (Fattuhi & Hughes, 1988). The main acidifying agent of acid rain water consists mainly of sulphuric acid and nitric acid and has a pH value between 4.0 and 4.5, which may cause surface weathering of exposed concrete (Fattuhi & Hughes, 1988; Neville, 2011).

2.0 DETAILS EXPERIMENTAL

2.1 Materials and Procedures

Ordinary Portland cement (OPC), CEM I with strength of 42.5 MPa, conforming to ASTM C150 (2012) standard. The natural fine aggregates (river sand) and coarse aggregates (crushed gravel) were locally purchased in the market. The iron ore tailings was obtained from one iron ore mills in the southern State of Malaysia Peninsula. A superplasticizer comply with ASTM C494 (2013) was used to increase the workability of mix.

The chemical composition of river sand and IOT were determined using X-ray fluorescence (XRF) and the results are shown in Table 1.The physical properties of IOT showed that the specific gravity = 2.8, relative density = 1.27 g/cm^3, fineness modulus = 2.07 and water absorption rate = 7.0%. The of particle size distribution of the IOT material and river sand is shown in Table 2.

2.2 Thermo gravimetric and Differential Thermal Analysis (TGA/DTA)

The equipment used for the test is Mettler Toledo TGA/STDA 851^e thermo gravimetric analyser. The specimens were heated within a temperature range of 30.0 ± 2.0 °C to 1000 ± 2.0 °C at a heating rate of 10 °C min^{-1} and helium content of 10ml/min. Within the specified temperature range, the mass loss and the decomposition temperatures were determined, recorded and reported. The results of TGA/DTA curves of IOT and river sand are shown in Fig. 1 and 2, respectively.The thermal decomposition in IOT specimen was observed to be in three phases. It can be seen that the endothermic peak valley in IOT at phase I is between 40 °C and 140 °C are normally associated with loss of surface water and dehydroxylation of the material (Maifala & Tabbiruka, 2007). Two peaks of heat release appeared at 240 °C and 360 °C due to the oxidation reaction with 4.12% weight loss in this period. Meanwhile, the oxidation of hematite was also occurred in this temperature range, but the heat and weight variation were concealed by the stronger oxidation reaction. There was a weight loss of 1.43% in the sample at the temperature range of 700–1000 °C, which may be due to the decomposition of calcite into CaO at 760 °C (Cai et al., 2016) and dehydroxylation of quartz at 480–580 °C. The endothermic peaks of river sand at 80 °C and 180 °C were also due to the loss of surface water and dehydroxylation. The difference between the DTA temperatures due to endothermic reaction of the sand and that of the IOT shows a similar transition.

TGA curve further showed that the sample decomposed from 100% to 91.14% for IOT, which correspond to the mass loss of 6.15% and 2.71% due to the decomposition of adsorbed water between 40 to 140 °C and 230 to 360 °C, respectively, making loss of about 8.86%. However, river sand decomposed from 100 to 95.1% with a loss of about 4.9%. Comparing the values, IOT decomposed more than river sand when exposed to temperature, and this could be due to high porosity and loose nature of the particle.

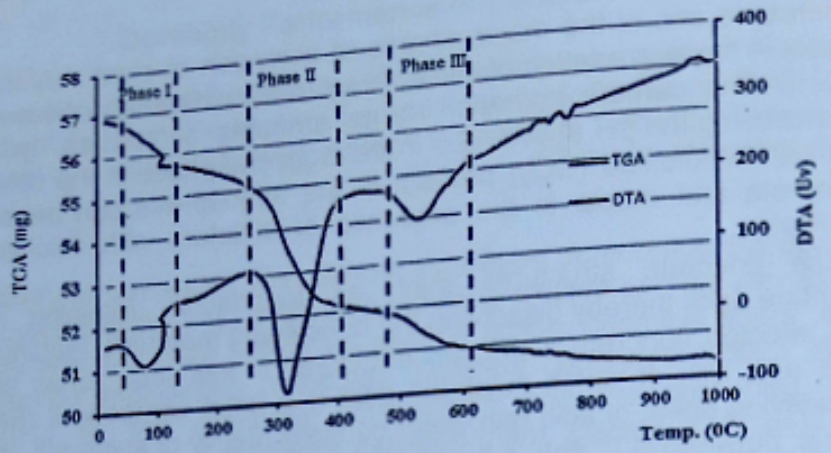

Fig. 1: Thermo Gravimetric and Thermal Differential Analyses IOT

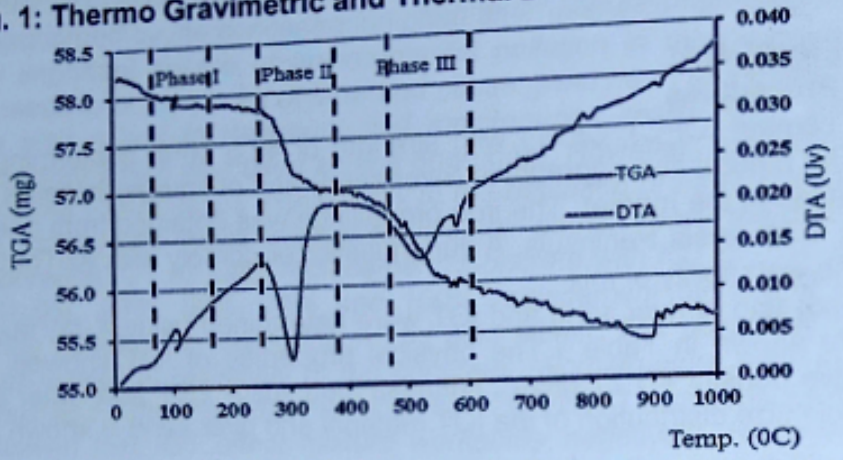

Fig. 2: Thermo Gravimetric and Thermal Differential Analyses River sand

Table 1: Chemical composition of river sand and iron ore tailings

Chemical composition (%)	SiO	Al_2O_3	Fe_2O_3	CaO	MgO	MnO	K_2O	CUO	ZnO	PbO	SO_3	LOI
River Sand	98	0.4	0.1	0.9	0.2	0.02	1.4	-	-	-	-	0.1
IOT	56	10	8.3	4.3	-	1.7	1.5	0.2	0.1	0.4	-	3.3

Table 2: Results for Sieve analysis of IOT material and river sand

	Iron ore tailings		River sand	
B.S.SIEVE SIZE (mm)	PERCENTAGE PASSING	PERCENTAGE RETAINED	CUMMULATIVE PERCENTAGE PASSING	CUMMULATIVE PERCENTAGE RETAINED
10	100	0	100	0
5.0	99.6	0.4	97.8	2.2
2.36	97.8	2.2	88.6	11.4
1.18	94.1	5.9	67.0	33.0
0.60	70.5	29.5	42.2	57.8
0.30	24.7	75.3	20.2	79.8
0.15	5.9	94.1	7.2	92.8
PAN	0	0	0	0
FINENESS MODULUS		2.07		2.77

2.2 Mix proportion

The Department of the Environment (DOE, 1992) method of concrete mix design was used to obtain the mix proportions required to produce concrete of grade C60 and C30 MPa at 0.40 and 0.60 w/c ratios, respectively. Considering the high water absorption of IOT Superplasticizer (SP) was used to achieve the required workability. The designations, proportions, and some properties of the concrete mixtures are given in Table 3 and 4.

In Table 3 the control mix of 0% IOT was designated as MT-1 and mixes made with 25%, 50%, 75% and 100% IOT were designated with MT-2, MT-3, MT4 and T-5 respectively. Similarly in Table 4 control mix of 0% IOT, having 0.60 w/c ratios was designated as MT-6 and mixes with 25%, 50%, 75% and 100% IOT were designated MT-7, MT-8, MT-9 and T-10, respectively.

Table 3: Mix proportion of concrete at 0.40 w/c

Properties	MT-1	MT-2	MT-3	MT-4	MT-5
OPC (kg/m^3)	480	480	480	480	480
Coarse aggregate (kg/m^3)	983	983	983	983	983
Natural sand (kg/m^3)	712	534	356	178	-
Iron ore tailings (kg/m^3)	-	178	356	534	712
Water (kg/m^3)	18	190	180	180	180
Superplastizer (%)	1.0	1.0	1.0	1.0	1.0
Slump (mm)	110	105	95	90	75
Compressive Strength (Mpa) at 90 day	64.5	66.8	68.6	67.0	66.3

Table 4: Mix proportion of concrete at 0.60 w/c

Properties	MT-6	MT-7	MT-8	MT-9	MT-10
OPC (kg/m^3)	380	380	380	380	380
Coarse aggregate (kg/m^3)	1009	1009	1009	1009	1009
Natural sand (kg/m^3)	761	571	380.5	190	-
Iron ore tailings (kg/m^3)	-	190	380.5	571	761
Water (kg/m^3)	230	230	230	230	230
Superplastiizer (%)	0.5	0.5	0.5	0.5	0.5
Slump (mm)	130	110	100	90	80
Compressive Strength (Mpa) at 90 day	39.5	42.9	50.3	45.1	43.9

2.3 Specimens casting and curing

For each concrete mixture, 100mm cubes and 100 x 200mm cylinders were cast. The cubes were used to determine the compressive strength and acid resistance test while the cylinders for rapid chloride penetration, accelerated carbonation tests and electrical resistivity test. All the specimens were demoulded 24 h after casting and were cured under water at $27^0 \pm 2^0$ C until the test age.

2.5. Test Method

The durability tests conducted include: Carbonation test, Rapid chloride penetration, acid resistance test, concrete electrical resistivity and corrosion measurements using LPR method.

2.5.1 Rapid Chloride Penetration Test

Rapid chloride penetration test (RCPT) was conducted in accordance with ASTM C1202 (2012) to determine the chloride ions charge into the concrete specimen. A 50 mm thick sliced of 100 mm were cut from 200 mm length of cylindrical specimen cured for 7, 28 and 90 days. The specimen were conditioned by vacuum saturation, and enclosed in a cell flanked by reservoirs that contains 0.3 M NaOH solution on one side and 3% NaCl solution on the other. A 60V potential difference was applied between the electrodes placed on both faces of the specimen, for a period of 6 hrs. The current passed were measured at the interval of 30 minutes for the 6 hours period using data logger.

2.5.2 Accelerated Carbonation test

The carbonation test was carried out in accordance with the method used by Chang and Chen (2006) and in line with RILEM-CPC-18 (2011) guidelines. In this test method, the specimens were exposed to accelerated carbonation in a carbonation Chamber. Two concrete cylinders with a diameter 100 x 200 mm specimens were tested for each of the respective mixes. After 90 days of storage in the CO_2 chamber, the samples were split into half and 1% phenolphthalein solution was sprayed on cross sections of the cubes. After spraying the solution, the un-carbonated area changes colour to purple, while the carbonated area remains colourless. The average carbonation depth of the specimen was determined by measuring the distance between the purple colour boundary and the edge of the specimen.

2.5.3 Acid Resistance test

Concrete cube of 100 mm for control and IOT concretes were immersed into 2.5% diluted sulphuric acid (H_2SO_4) solution (pH = 1) and a temperature of 23.0 ± 2.0 °C. Prior to immersion the cube specimen were wiped to surface dry and weighed to the nearest gram using electronic weighing balance and this was noted as the reference weight. Visual observations of acid attack on specimens and weight losses were determined at 7, 28 and 90 days of immersion

2.5.4 Electrical resistivity test

The test for the surface electrical resistivity of the concrete was carried out using Resipod SFE 2011.03.31 high resolution electric resistivity meter. The test was carried out using the four-point Wenner array probe technique in accordance with AASHTO-TP-95-11, (2011). The test was carried out on adequately cured and saturated surface of cylindrical concrete diameter of 100 × 200 mm at 7, 28 and 90 days.

3. RESULTS AND DISCUSSION

3.1. Rapid chloride penetration test (RCPT)

The results of rapid chloride ion penetration measured in terms of the electric charge passed in coulombs through the respective concrete specimens cured at the ages of 7, 28 and 90 days are presented in Table 4 and 5 for 0.40 and 0.60 w/c ratios, respectively. From Table 5, it can be seen that at 7 days the total coulomb charge passed through the specimens were higher compared to 90 days. From the result it can be observed that the coulomb charge of the entire specimens at 7 days falls within the moderate classification range 1000-2000 Coulombs of chloride ion penetrability (ASTM C1202, 2012), which indicated low penetrability of ions charge. However, the charge of ions for all specimens decreased at 90 days of curing and falls within 100 -1000 Coulombs, which was classified as very low penetrability.

Similarly, it can be seen from Table 6 that the entire set of values decreases the rate of penetration of chloride charge ions as the curing age increases. The total coulomb charge passing through the specimens at 90 days are 1100, 1134, 1219, 1356 and 1875 for MT-6, MT-7, MT-8, MT-9 and MT-10 concrete, respectively. These values also fall within low classification (1000-2000 Coulombs) chloride ion penetrability based on ASTM C1202. As the curing ages increased the coulomb charge in concrete containing IOT reduces rapidly when compared with that of control concrete. In general, the permeability of concrete containing IOT was higher compare to control specimens. The higher charge in IOT could be attributed to the high water absorption of the IOT concrete. The higher alumina content of IOT material as seen in the chemical composition (Table 1) cannot resist the forced penetration of chloride-ions, hence concrete permeability increased. The replacement of river sand with 100% IOT in concrete has an intense effect on the depth of chloride penetration of concrete.

Table 5: RCPT test results of 0.40 w/c ratio

Curing Age (days)	Charge passed (coulombs)				
	MT-1	MT-2	MT-3	MT-4	MT-5
7	1297	1314	1362	1371	1590
28	1000	1108	1138	1206	1238
90	839	849	871	876	886

Table 6: RCPT test results of 0.60 w/c ratio

Curing Age (days)	Charge passed (coulombs)				
	MT-6	MT-7	MT-8	MT-9	MT-10
7	1270	1445	1688	1754	2284
28	1108	1226	1473	1570	1993
90	1100	1134	1219	1356	1875

3.2 Accelerated carbonation depth

The Fig. 3 shows that concrete specimens that were carbonated was indicating colourless to the purple-red colour of phenolphthalein at the edge of the specimens, while concrete specimen of un-carbonated indicates purple-red colour of phenolphthalein showing resistance to carbonation within the period of 90 days of exposure. The depth of carbonation for all these specimens within this period were virtually equal to zero. This could be attributed to none interconnected pores that will facilitate the ingress of CO_2. The use of lower water-cement ratio also reduces the porosity of the concrete. In a related findings, Basheer, Russell, and Rankin (1999) reported that the rate of carbonation of concrete is primarily influenced by the water-cement ratio, porosity and carbon dioxide transport.

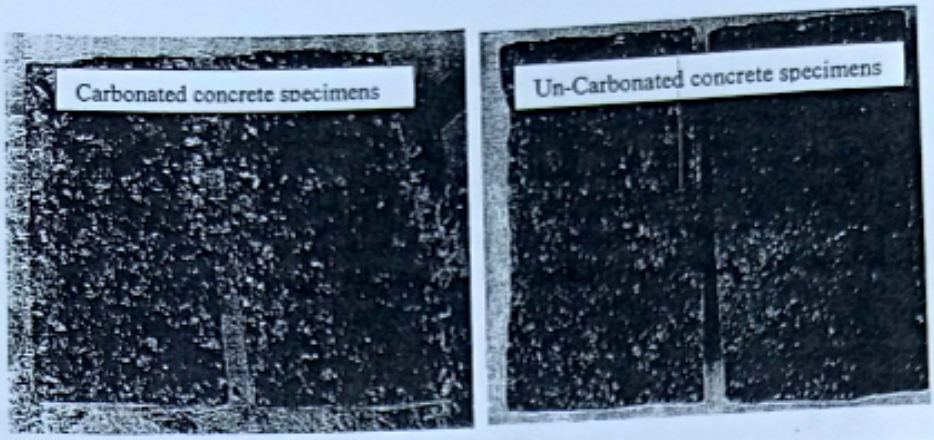

Fig. 4 shows the results of carbonation test conducted on the concrete specimens of 0.60 w/c ratio. It is observed that the mean carbonation depth decreased as the percentage of IOT in concrete mixes increased, thus, presenting a better performance throughout the replacement of river sand. Similarly Siddique, Aggarwal, Aggarwal, Kadri, and Bennacer (2011) observed that, concrete with foundry sand mixes showed good resistance to carbonation. This reduction in carbonation depth in the concrete specimens containing IOT might be due to the micro-pore filling with finer particles of IOT which could not facilitate the access of CO_2.

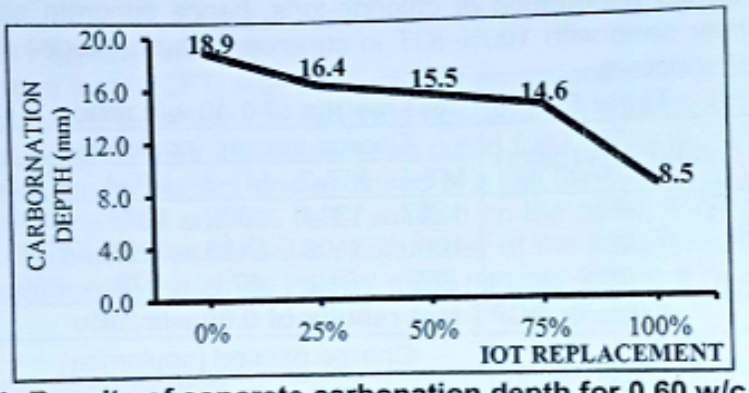

Fig. 4: Results of concrete carbonation depth for 0.60 w/c ratio

3.3 Resistance to Acid Attack

The results of the weight loss of the respective concrete mixes due to sulphuric acid attack are presented in Table 7. It is observed that all the specimens exhibited the same trend of decrease in mass throughout the period of 7, 28 and 90 days of immersion. This mass loss is brought about by the action of the acid which reacts with calcium hydroxide to damage the cement gel binder of concrete (Bakharev, Sanjayan, & Cheng, 2003) and forms white, soft and soluble gypsum on the surface. Throughout the period of exposure, the weight of concrete containing IOT decreased more than the controls. As can be seen in the two figures, the results indicate an increase in weight loss for 0.60 w/c ratio in comparison to 0.40 w/c ratio. IOT containing MT-100 concrete exhibited the highest weight loss of 5.24%. On the other hand, control specimen, MT-6 exhibited the least weight loss of 0.91% at the same period of 90 days. The higher weight loss of IOT concrete could be attributed to the permeability of IOT concrete with reference to water absorption and difference in chemical and phase composition. The IOT material had calcium as observed in the chemical composition, which has strong reactions with sulphuric acid and weaken the concrete matrix. Similar finding was reported by Singh, Siddique, Ait-Mokhtar, and Belarbi (2016) on concrete with high volumes of low-calcium coal bottom ash exposed to sulphuric acid. Another destructive action of acid is the reaction between calcium and higher aluminate in the IOT composition forming the less soluble reaction product ($3CaO.Al_2O_3.32H_2O$). This very expansive compound causes internal pressure in concrete, which results in the swelling, formation of cracks and surface softening (as shown in Fig. 5) and results in loss of mechanical strength of concrete.

Table 7: Weight loss of various concretes due to acid attacked

Concrete specimen	Weight loss (%)			w/c ratio
	7d	28d	90d	
MT-1	0.21	0.56	0.91	0.40
MT-2	0.42	1.03	1.25	
MT-3	0.83	1.41	2.00	
MT-4	1.08	1.92	2.01	
MT-5	1.1	1.83	2.39	
MT-6	1.05	1.84	2.51	0.60
MT-7	1.55	1.9	3.95	
MT-8	2.38	3.32	5.00	
MT-9	2.42	3.35	5.14	
MT-10	2.48	3.45	5.24	

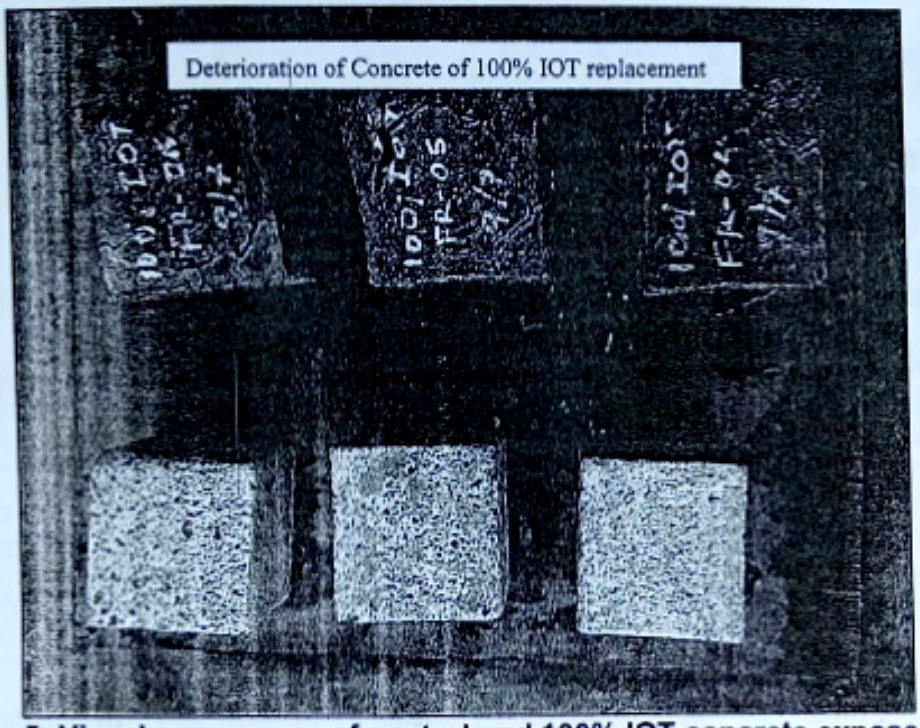

Fig. 5: Visual appearance of control and 100% IOT concrete exposed to

3.4 Concrete electrical resistivity

The concrete electrical resistivity has proven to be an effective parameter for the estimation of the corrosion risk of steel reinforcement in concrete. The average test results of the concrete resistivity of the concrete specimens are presented in Table 8. It can be seen from the table that the concrete resistivity of the respective concrete range from 5.1 to 15.2 kΩcm. The electrical resistivity of concrete should be greater than 8.5 kΩ-cm, since the corrosion rate have been found to be high below this limit (Hope, Page, & Ip, 1986). Similarly, Morris, Vico, Vazquez, and de Sanchez (2002) reported that reinforcing steels in concrete are likely to achieve an active state of corrosion when concrete is lower than 10 KΩcm, and likely to present a passive behaviour when concrete resistivity is higher than 30 KΩcm.

Generally, concrete is said to exhibit moderate to low corrosion rate when its true electrical resistivity is between 5 and 10 kΩ-cm, whereas good corrosion resistance is achieved when the true electrical resistivity is above 10 kΩ-cm (Neville, 2011). In this study, all the test results with 0.40 w/c ratio shows that concrete resistivity were higher than 10 kΩcm. Meanwhile, concrete resistivity values for 0.60 w/c ratio at 90 days are less than 10 kΩcm. However, the value for 50% (MT-8) replacement has satisfied the minimum limit of 8.5 kΩcm recommended by Hope, Ip, and Manning (1985). The water-cement ratio and curing period of concretes have significant effect on

concrete resistivity. Similar effects of water-cement ratio on electrical resistivity were reported by Hossain (2005) that the resistivity of concrete usually increases with lower porosity and smaller pore size because the flow of ions through the pore spaces becomes hindered.

Table 8: Variation in electrical resistivity of the concretes with curing age

Concrete specimen	Concrete resistivity (KΩcm)			w/c ratio
	7d	28d	90d	
MT-1	13.4	14.3	15.2	0.40
MT-2	15.7	14.4	14.6	
MT-3	12.7	13.9	15.0	
MT-4	12.3	13.2	15.3	
MT-5	9.8	12.4	12.6	
MT-6	9.1	10	10	0.60
MT-7	5.6	6.5	7.8	
MT-8	7.6	8.1	9.0	
MT-9	5.4	6.8	7.8	
MT-10	5.1	6.2	6.9	

CONCLUSIONS

Based on the experimental investigation, the following conclusions were highlighted:

1. The rapid chloride penetration test values indicated that IOT concretes have high flow of electric charge at 7 days compared to control concrete. But as the duration of curing increased, the chloride ions penetration were decreased. This decrease can be attributed to the reduction in permeation resulting from the pore refinement of the concrete.
2. The performance of concrete containing IOT exposed to carbon dioxide environment, showed excellent resistance to rapid carbon dioxide penetration up to 90 days of exposure.
3. Negative mass change was observed in the IOT concrete due to the reaction between the sulphuric acid and calcium in IOT material forming calcium carbonate.
4. The electrical resistivity test results also indicated that concrete containing IOT exhibited lower electrical resistivity than the control at 0.60 w/c ratio. Although both the control and the IOT concretes showed good electrical resistivity values at 0.40 w/c ratio and they were classified with low corrosion tendency.

ACKNOWLEDGMENT

The authors are grateful to Federal Government of Nigeria through Tertiary Education Trust Fund (Tetfund) and Universiti of Teknologi Malaysia, where the experimental work and the analysis were carried out.

REFERENCE

ASTM C150. (2012). American Standard Testing of Materials -Standard Specification for Portland Cement. *American society of testing and materials Publication*. doi: 10.1520/c0150_c0150m-12

ASTM C494. (2013). American Standard Testing of Materials - Standard Specification for Chemical Admixtures for Concrete. *American society of testing and materials Publication*, 10. doi: 10.1520/c0494_c0494m-13

ASTM C1202. (2012). American Standard Testing of Materials - Standard Test Method for Electrical Indication of Concrete's Ability to Resist Chloride Ion Penetration. *American society of testing and materials Publication*. doi: 10.1520/c1202-12

Bakharev, T.; Sanjayan, J. G., & Cheng, Y. B. (2003). Resistance of alkali-activated slag concrete to acid attack. *Cement and Concrete Research, 33*(10), 1607-1611. doi: 10.1016/s0008-8846(03)00125-x

Basheer, P. A. M., Russell, D. P., & Rankin, G. I. B. (1999). *Design of concrete to resist carbonation*. Paper presented at the Durability of Building Materials and Components Ottawa ON, K1A 0R6, Canada. 423-435.

Cai, L., Ma, B., Li, X., Lv, Y., Liu, Z., & Jian, S. (2016). Mechanical and hydration characteristics of autoclaved aerated concrete (AAC) containing iron-tailings: Effect of content and fineness. *Construction and Building Materials, 128*, 361-372. doi: 10.1016/j.conbuildmat.2016.10.031

Chang, C.-F., & Chen, J.-W. (2006). The experimental investigation of concrete carbonation depth. *Cement and Concrete Research, 36*(9), 1760-1767. doi: 10.1016/j.cemconres.2004.07.025

Fattuhi, N. I., & Hughes, B. P. (1988). The Performance of Cement Paste and Concrete Subjected to Sulphuric Acid. *Cement and Concrete Research., 18*, 545-553.

Hope, B. B., Ip, A. K., & Manning, D. G. (1985). Corrosion and electrical impedance in concrete. *Cement and Concrete Research, 15*(3), 525-534. doi: http://dx.doi.org/10.1016/0008-8846(85)90127-9

Hope, B. B., Page, J. A., & Ip, A. K. C. (1986). Corrosion rates of steel in concrete. *Cement and Concrete Research, 16*(5), 771-781. doi: https://doi.org/10.1016/0008-8846(86)90051-7

Hossain, K. M. A. (2005). Correlations between porosity, chloride diffusivity and electrical resistivity in volcanic pumice-based blended cement pastes. *Advances in Cement Research, 17*(1), 29-37.

Khunthongkeaw, J., Tangtermsirikul, S., & Leelawat, T. (2006). A study on carbonation depth prediction for fly ash concrete. *Construction and Building Materials, 20*(9), 744-753. doi: 10.1016/j.conbuildmat.2005.01.052

Maifala, B., & Tabbiruka, N. M. S. (2007). Chemical and thermal characterization of a clayey material found near Gaborone Dam. *Applied Science Environmental Management, 11*(4), 77 - 80.

Morris, W., Vico, A., Vazquez, M., & de Sanchez, S. R. (2002). Corrosion of reinforcing steel evaluated by means of concrete resistivity measurements. *Corrosion Science, 44*(1), 81-99. doi: http://dx.doi.org/10.1016/S0010-938X(01)00033-6

Neville, A. M. (2011). *Properties of concrete*. London: Pearson Education Limited.

RILEM-CPC-18. (2011). Measurement of hardened concrete carbonation depth. *Technical Committee TDC for Compilation of Test Methods to Determine Durability of Concrete*, 11.

Siddique, R., Aggarwal, Y., Aggarwal, P., Kadri, E.-H., & Bennacer, R. (2011). Strength, durability, and micro-structural properties of concrete made with used-foundry sand (UFS). *Construction and Building Materials, 25*(4), 1916-1925. doi: 10.1016/j.conbuildmat.2010.11.065

Singh, M., Siddique, R., Ait-Mokhtar, K., & Belarbi, R. (2016). Durability Properties of Concrete Made with High Volumes of Low-Calcium Coal Bottom Ash As a Replacement of Two Types of Sand. *JOURNAL OF MATERIALS IN CIVIL ENGINEERING, 28*(4), 04015175. doi: 10.1061/(asce)mt.1943-5533.0001464

Yang, C. C., & Chiang, S. C. (2008). A Rapid Method for Determination of the Chloride Migration. *Journal of ASTM International, 5*(4).

Yaprak, H., Aruntas Huseyin Yılmaz, Demir Ilhami, Simsek Osman, & Gokhan., D. (2011). Effects of the fine recycled concrete aggregates on the concrete properties. *International Journal of the Physical Sciences, 6*(10), 2455-2461. doi: 10.5897/ijps11.253